J. Membrane Biol. 32, 75–92 (1977)

Spatial Distribution of Functional OH^- Carriers Along a Characean Internodal Cell: Determined by the Effect of Cytochalasin B on $H^{14}CO_3^-$ Assimilation

William J. Lucas and Jack Dainty

Department of Botany, University of Toronto, Toronto M5S 1A1, Ontario, Canada

Received 30 June 1976

Summary. The present study was aimed at testing an hypothesis relating to the OH^- efflux pattern developed on internodal cells of *Chara corallina*. It was suggested that OH^- efflux carriers were restricted to a limited number of sites along the internodal cell. Hydroxyl ions were considered to be delivered to these sites via the streaming cytoplasm. To test this hypothesis, cytochalasin B was used to inhibit cyclosis. Under these conditions OH^- efflux and $H^{14}CO_3^-$ assimilation should have been inhibited.

Our results indicated that cyclosis was inhibited within 60 min in the presence of 30 μg/ml cytochalasin B. When $^{14}CO_2$ (pH 5.0) fixation experiments were conducted under these conditions, no inhibition of photosynthesis was observed. Cytochalasin B was shown, therefore, to inhibit cyclosis without affecting the *in vivo* reactions of photosynthesis.

A parallel study on the effect of increasing cytochalasin B concentrations on cyclosis and $H^{14}CO_3^-$ assimilation revealed that there was a limiting velocity of cyclosis below which $H^{14}CO_3^-$ assimilation was inhibited. These results were interpreted in terms of a rate-limiting step associated with the supply of OH^- to the operational efflux sites.

At cytochalasin B concentrations below 15–20 μg/ml, no effect was observed on $H^{14}CO_3^-$ assimilation. This suggested that cytochalasin B does not interfere with the membrane-bound HCO_3^- and OH^- transport systems of this species.

The OH^- efflux pattern underwent significant modification following cyclosis inhibition. A change from discrete band efflux sites to a network of numerous small, localized, disc-shaped efflux sites was observed. The discovery of this modified OH^- efflux system provided an explanation for the observed limited sensitivity of $H^{14}CO_3^-$ influx to cessation of cyclosis.

These results invalidated part of our hypothesis, since they revealed that the OH^- carriers are uniformly distributed over the plasmalemma surface. A modified hypothesis to account for the spatial distribution of the OH^- efflux sites is presented.

Several Characean species (giant fresh water algae cells) develop light-dependent acid and alkaline bands along their cell walls [20, 19, 15]. The alkalinization phenomenon depends upon the presence of exogenous HCO_3^- in the experimental solution [15]. Photosynthetic assimilation of the carbon supplied by HCO_3^- results in the production of one OH^- for each CO_2 molecule fixed. This "waste product" (OH^-) is exported

from the cytoplasm, across the plasmalemma, at discrete OH^- efflux sites [11, 12]. Each alkaline band is formed by the transport of OH^- over a small cylindrical band of plasmalemma surface [11], the length of which is approximately 0.05 cm (cf. 4–5 cm total cell length). Accumulation of OH^- at the cell surface, and its diffusion into the neighboring bathing solution, gives rise to the observed alkaline banding phenomenon [15, 11].

Under HCO_3^- assimilating conditions, the OH^- bands are spaced at somewhat regular intervals along the length of the internodal cell. The number of bands per cell and their efflux activities depend on the level of exogenous HCO_3^-, the incident light intensity and the length of the actual cell [15, 11, 12]. Recent progress in this field has revealed that the OH^- efflux system of *Chara corallina* is, however, a more complex phenomenon than would appear at first sight [11, 12, 14]. There exists an hierarchy of functional OH^- efflux sites within the plasmalemma. The three operationally distinct forms of OH^- bands that have been observed were termed the primary, sub-primary and subsidiary OH^- efflux systems [12]. Within this hierarchy the primary OH^- efflux site always activates first and is the last to deactivate, under a given set of experimental conditions; the sub-primary behaves in an almost identical manner. It is thought the subsidiary sites activate only when the OH^- production rate, at the chloroplast layer, exceeds the combined efflux rates of the primary and sub-primary systems. Under these conditions subsidiary sites activate at various positions along the internodal cell, until the combined OH^- efflux activity of the operational bands equals the photosynthetic production of OH^- [12]. This system is a unique example of cytoplasmic substrate regulation on a macroscopic scale, i.e., the distribution of the OH^- efflux sites along the cell appears to be related to their capacity to efflux the photosynthetically generated OH^- from the chloroplast layer. (In these cells the chloroplasts are uniformly distributed in a single layer in the outer, nonstreaming cytoplasmic layer.)

As a result of these recent studies, we became interested in the question of the cellular mechanism controlling the spatial distribution of the primary, sub-primary and subsidiary OH^- bands along an internodal cell. This interest increased when it was discovered that the HCO_3^- and OH^- transport systems function independently, in that the respective ions are transported across the plasmalemma by different sets of carriers [14]. This suggested to us that in order to maximize photosynthesis, the HCO_3^- carriers would probably be uniformly distributed over the

cell membrane surface. A situation of this nature would involve complex electrical and transport interactions between the two systems, especially as the OH^- efflux system is so highly localized.

This system was investigated in the present study, and on the basis of our results we have formulated a model which we feel can account for the spatial distribution of the OH^- efflux sites of *C. corallina*.

Materials and Methods

Chara corallina cells were cultured in the laboratory under artificial light. Culture details and the method used to cut internodal cells from the culture have been previously reported [15, 13]. In general, mature third to fifth internodal cells were used.

The standard experimental solution contained 1.0 mM NaCl, 0.2 mM KCl and 0.5 mM $CaSO_4$, unless otherwise specified. The pH values of some solutions were controlled by artificial buffers. All chemicals used were of Analar Reagent grade.

Radioactive $NaH^{14}CO_3$ was obtained from New England Nuclear, Boston, as a sterile aqueous solution, and aliquots were added to the experimental solutions to give a final specific activity of 1 mCi per mmole.

Cytochalasin B was obtained from Aldrich Chemical Company, Milwaukee, Wisconsin. A stock solution (3 mg/ml) in dimethyl sulphoxide (spectroscopic grade) was stored at 4 °C until used. This stock solution was added to experimental media to give the concentrations described in the text. Unless otherwise specified, the final dimethyl sulphoxide concentration in experimental and control solutions was 1% (v/v).

Cytoplasmic streaming and radioisotope ($NaH^{14}CO_3$) studies were performed on cells cut one day prior to the actual performance of the experiment. These cells were pre-treated in experimental solution which contained 1.0 mM $NaHCO_3$ (pH 9.0). The light regime employed for the cultures (13L:11D) was maintained during this pre-treatment period, and all cells were illuminated under fluorescent lights (10 Wm^{-2}) for 2 hr prior to the commencement of an experiment. For experiments associated with cytochalasin B, a 1 hr pre-treatment in 1% dimethyl sulphoxide was employed. The actual duration and radioactive exposure period for each experiment is indicated in the text. The radioisotope techniques employed have been detailed by Lucas [13]. Cyclosis was measured with a binocular microscope having an ocular micrometer. The time required for a standard sized cytoplasmic particle to traverse 1000 μm was measured with a stopwatch; 10 cells were used per treatment. (When cyclosis was severely retarded, the traverse distance was reduced to 100 μm.)

Details of the illumination and experimental systems have been previously reported [12].

The pH values along the cell surface of *C. corallina* internodal cells were measured using the technique developed by Lucas and Smith [15]. To prepare agar blocks (0.7% w/v) containing cytochalasin B and/or 1.0 mM $NaHCO_3$, the following procedure was employed. Agar powder (Difco, Bacto-agar) was dissolved by boiling a known volume of standard experimental solution. This solution was then cooled to 39 °C, at which temperature the required amounts of stock $NaHCO_3$ and cytochalasin B solutions were added. The pH value was checked and titrated to the required value. Agar blocks were then set within perspex holders. Channels designed specifically to hold experimental *Chara* cells, were made in the agar blocks [13] and cells subsequently located in them. The blocks were then placed in thermostatted experimental solutions. Following a 2 hr illumination period, a Leitz micromanipulator was used to traverse a miniature pH electrode (Microelectrodes, Inc., Model MI-405) along the cell wall. From the values obtained the pH pattern established was mapped.

Results and Discussion

A Working Hypothesis

The simplest explanation for the localized, regular pattern of OH^- efflux sites along a particular *Chara* cell was that the transport entities (carriers) are restricted to a limited number of sites along the length of the plasmalemma. In addition, we also considered that the HCO_3^- transport system was uniformly distributed (on a macroscopic scale) over the entire plasmalemma surface.

At this point it should be stressed that these cells are, to a good approximation, right circular cylinders of macroscopic dimensions (diameter 0.6–1.0 mm, length 40–80 mm), having their chloroplasts restricted to a single uniform layer in the outer region of the cortical (gel) cytoplasm. The distance from the plasmalemma to the chloroplast layer is approximately 4–6 μm [5]. Consequently, the time associated with the diffusion of HCO_3^- from the carriers to the chloroplasts would be extremely short (approximately 50–200 msec). However, the lateral diffusion path from the site of OH^- generation, within the chloroplast layer, to the nearest operational OH^- efflux site can be quite long. The distance between neighboring operational OH^- efflux sites, under maximal HCO_3^- assimilating conditions, ranges from 6 to 10 mm (*see* Fig. 6A). The maximum lateral diffusion path for OH^- under these conditions would be 3–5 mm. But, when only the primary site is functioning, this distance can be 30 mm of more [12]. Free diffusion of OH^- over these distances would take a considerable time (approximately 1–50 hr respectively). It therefore seemed most likely that OH^- ions are not moved exclusively by free diffusion, but rather are rapidly transported around the cell by the streaming layer of the cytoplasm. (For a streaming rate of 60 μm per sec, the time to cover 5 and 20 mm is approximately 1.4 and 5.6 min, respectively.)

A prediction, based on the above, is that if cytoplasmic streaming is stopped, the rate of HCO_3^- assimilation should be greatly reduced. The OH^- efflux process would be expected to be rate-limiting under these conditions, since HCO_3^- influx cannot proceed for long in the absence of OH^- efflux.

Influence of Dimethyl Sulphoxide on Cyclosis and Photosynthesis

Cytochalasin B, an alkaloid metabolite of the fungus *Helminthosporium dematioideum* [1] inhibits cyclosis in the Characeae [21–23, 2, 4].

Table 1. Influence of Dimethyl Sulphoxide on ^{14}C assimilation[a]

pH Value of experimental solution	Exogenous substrate	Assimilation of ^{14}C (pmole cm^{-2} sec^{-1})	
		Control	1% Dimethyl sulphoxide
5.01	$^{14}CO_2$	116.4±5.0	123.1±5.9
9.00	$H^{14}CO_3^-$	62.2±1.9	60.2±2.3

[a] Radioactive ^{14}C assimilation was measured using a 1 hr pre-treatment, followed by a 1 hr exposure to the radioisotope solution. A concentration of 1.0 mM total carbon was employed at the two pH values. Experimental solutions at pH 5.01 were buffered by 5 mM 2-(N-morpholino) ethanesulphonic acid (MES); at pH 9.0 no artificial buffers were used. Values given are mean ± SEM (15 cells per treatment).

Although the recent literature relating to this compound indicates that it is not as specific in its action as previously thought [6], it was considered more reliable than compounds like *p*-chloromercuribenzoate [7] or 8-Hydroxyquinoline (W.J. Lucas, *unpublished*) and was consequently used in the present study.

Preliminary experiments were conducted to ensure that dimethyl sulphoxide, the solvent used for cytochalasin B, did not have a deleterious effect on either cyclosis or photosynthesis. Table 1 shows that 1% (v/v) dimethyl sulphoxide does not affect either $^{14}CO_2$ or $H^{14}CO_3^-$ assimilation. Similarly no effect was observed on cyclosis; this agrees with the findings of Williamson [22] and Bradley [2].

Inhibition of Cyclosis by Cytochalasin B

The nature of the time course of cyclosis inhibition by various cytochalasin B concentrations is shown in Fig. 1. The slow, linear phase of these time courses is indicative of a diffusion limited system. This is readily accounted for in this experimental system since stagnant solutions were employed throughout [16], and this would cause a diffusional limitation on the rate of entry of cytochalasin B to the cytoplasm. However, the results presented in Fig. 2 demonstrate that the time course of cyclosis inhibition is also strongly influenced by the level of dimethyl sulphoxide employed. Hence, since dimethyl sulphoxide probably acts both as a solvating agent and as a carrier for cytochalasin B across the plasmalemma, it would appear that the entry of cytochalasin B into the cell is limited by its permeation across the plasmalemma as well as by diffusion in the aqueous and cytoplasmic phases.

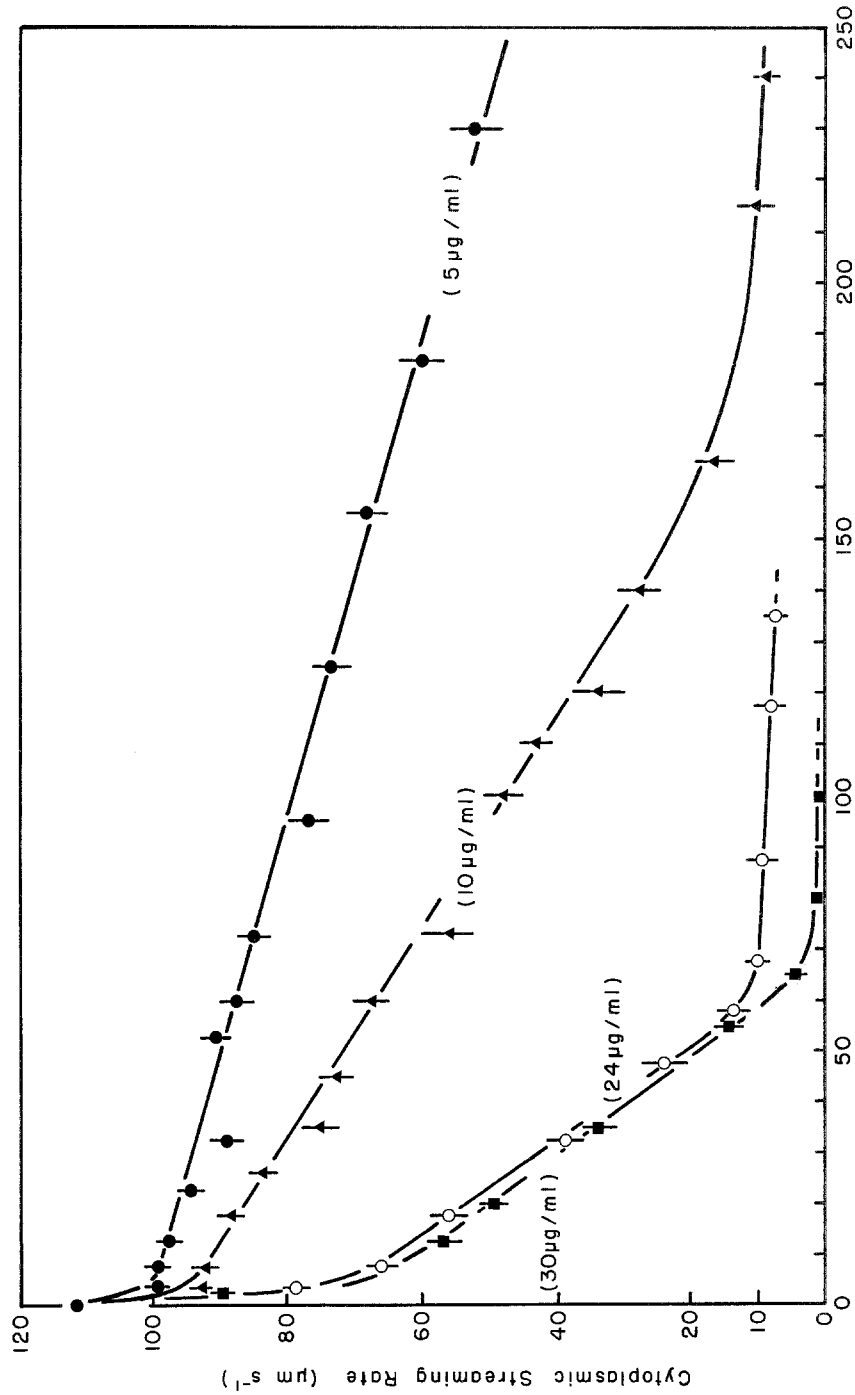

Fig. 1. Time course of cyclosis inhibition by cytochalasin B. Experiments were conducted in standard solutions, containing 1.0 mM $NaHCO_3$ (pH 9.0) and 1% (v/v) dimethyl sulphoxide, for 1 hr prior to transferring to solutions containing cytochalasin B. The actual cytochalasin B concentrations employed are indicated on the respective time courses. Ten cells were used for each time course and the values presented are the mean ± SEM

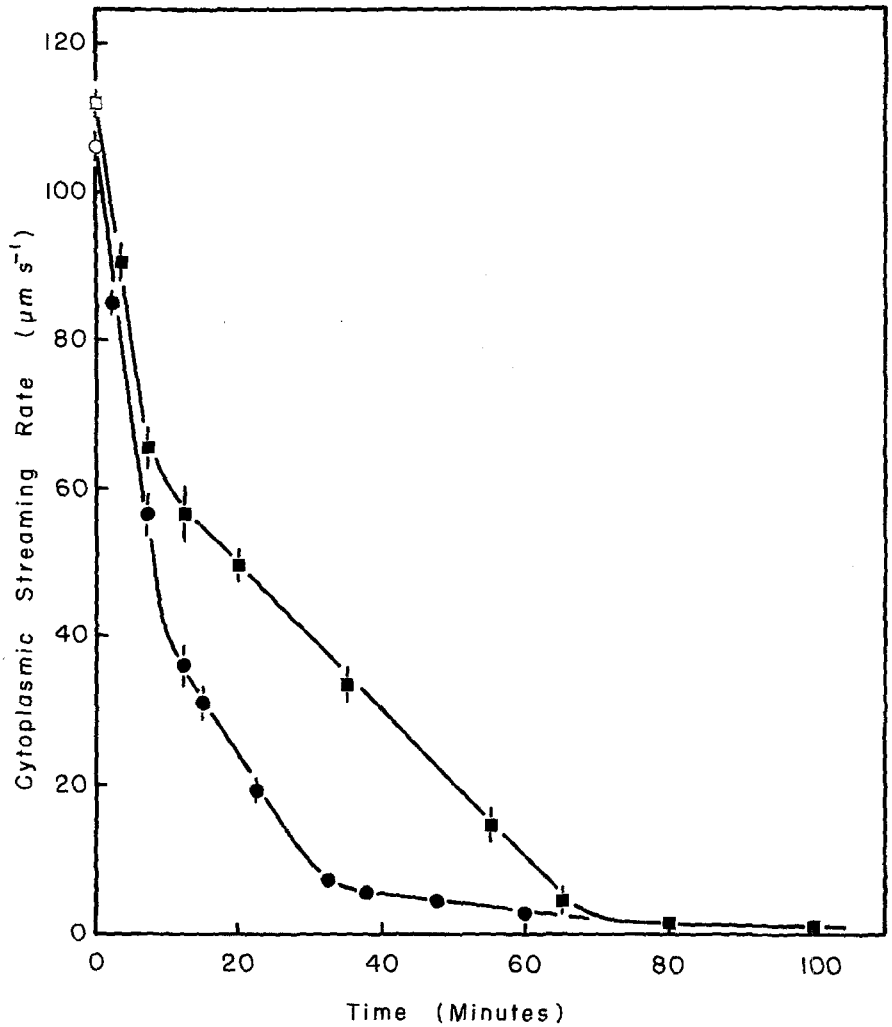

Fig. 2. Influence of dimethyl sulphoxide level on cytochalasin B mediated inhibition of cytoplasmic streaming. Experimental details are as in Fig. 1. The levels of dimethyl sulphoxide employed were 1% (■) and 2% (●) (v/v) and both treatments were conducted in the presence of 30 μg/ml cytochalasin B

Figs. 1 and 2 show that after a 70 min exposure to 30 μg/ml cytochalasin B, cytoplasmic streaming is reduced to a very low level. This concentration seemed suitable for investigating the effect of cytoplasmic streaming on $H^{14}CO_3^-$ assimilation. But, since exposure to this alkaloid during radioisotope and pH scanning experiments may extend to 100 min or longer, it was essential to ascertain whether the effect caused at this concentration was reversible. Fig. 3 demonstrates that it was reversible. Inhibition of streaming by 30 μg/ml cytochalasin B was found to be

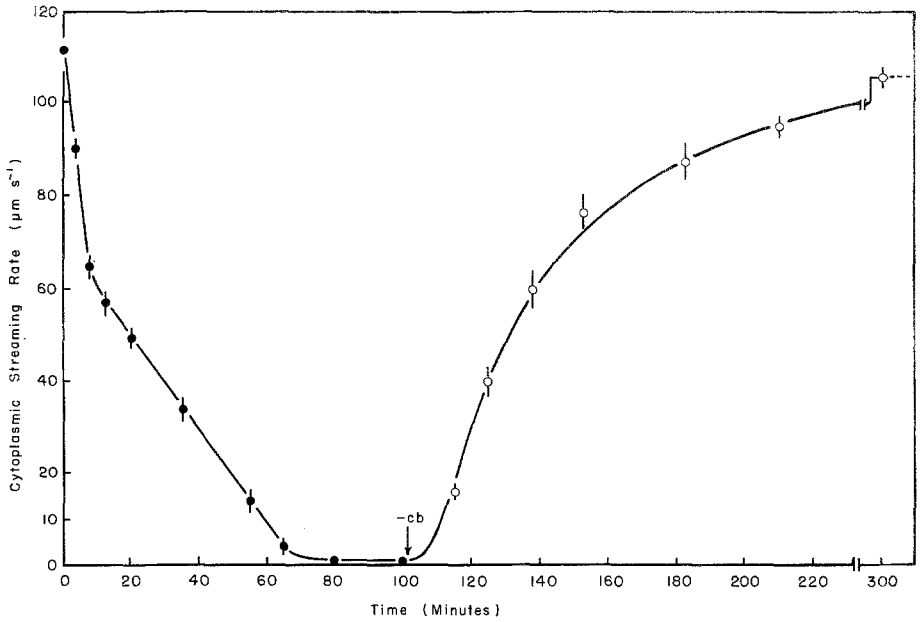

Fig. 3. Reversibility of cyclosis inhibition caused by cytochalasin B. Experimental details are as in Fig. 1. The experimental medium contained 30 μg/ml cytochalasin B (1%, v/v, dimethyl sulphoxide) for 102 min, a cytochalasin B-free medium was then substituted (−cb). This solution was changed three times in the first 10 min and then hourly

reversible for periods of up to 180 min, provided 1% (v/v) dimethyl sulphoxide was used. (Higher levels of dimethyl sulphoxide tended to decrease the reversibility.)

Effect of Cytochalasin B on $^{14}CO_2$ fixation

Exogenous CO_2 moves by passive diffusion from the external medium, through the plasmalemma and cortical (gel) cytoplasmic layer, to the chloroplasts. Consequently, over short periods when cyclosis is inhibited, the rate of CO_2 fixation should not be influenced by the inhibition of streaming, *per se*. Table 2 indicates that for periods up to 80 min, $^{14}CO_2$ fixation was not altered even though cyclosis was almost completely stopped. Therefore it can be assumed that cytochalasin B can inhibit streaming in *Chara* cells without affecting the reactions of photosynthesis.

Bicarbonate Assimilation in the Presence of Cytochalasin B

Fig. 4*A* and *B* represent the results of cyclosis and $H^{14}CO_3^-$ assimilation experiments conducted in parallel. An experimental cytochalasin

Table 2. Influence of 25 μg/ml Cytochalasin B on $^{14}CO_2$ fixation [a]

Experimental duration (min)	$^{14}CO_2$ fixation (pmole cm^{-2} sec^{-1})		Cyclosis (Percentage inhibition in presence of Cytochalasin B)
	Control	+ Cytochalasin B	
20	126.3 ± 4.2	123.6 ± 6.2	80.1
40	120.0 ± 4.0	115.9 ± 4.7	94.8
60	120.1 ± 9.0	127.1 ± 6.1	98.1
80	130.8 ± 3.4	123.1 ± 5.6	98.1

[a] Experimental solutions were buffered with 5 mM MES (pH 5.02) and contained 1.0 mM total carbon and 2% (v/v) dimethyl sulphoxide. Cytochalasin B concentration employed was 25 μg/ml. Following a 1 hr pre-treatment, nonradioactive experimental solutions were substituted until the final 20 min period of each treatment. Values are mean ± SEM (15 cells per treatment).

B exposure period of 1 hr was employed for this series of experiments. This period was chosen as it offered, by the use of various cytochalasin B concentrations, a wide range of cytoplasmic streaming rates, while all treatments would remain well within the reversible period of this drug (*see* Fig. 1). A decrease in cyclosis with increasing cytochalasin B concentrations was expected; however, the linear nature of the decline was not anticipated (Fig. 4*A*). We do not have a satisfactory explanation for this relationship.

Fig. 4*B* indicates that incomplete inhibition of $H^{14}CO_3^-$ assimilation (approximately 50%) occurred at high cytochalasin B concentrations, where cyclosis was completely inhibited. This aspect of the results will be discussed and expanded in a later section. The insensitivity of $H^{14}CO_3^-$ assimilation to cytochalasin B concentrations of up to 15 μg/ml is of importance, since it tends to eliminate the possibility that cytochalasin B caused the observed $H^{14}CO_3^-$ inhibition by an effect on the HCO_3^- transport system of the plasmalemma (*see* Fig. 4*B*). We interpreted the decrease in $H^{14}CO_3^-$ influx, under 20–35 μg/ml cytochalasin B, as resulting from the reduction of cyclosis below a "limiting velocity", i.e., below this "limiting velocity" the rate at which OH^- ions are supplied to the efflux sites becomes the limiting step in the overall process of $H^{14}CO_3^-$ assimilation. Based on the results presented in Fig. 4, the "limiting velocity" for these cells would be 38 ± 8 μm per sec.

To test this "limiting velocity" proposal, $H^{14}CO_3^-$ assimilation time course experiments were conducted at a 30 μg/ml cytochalasin B concentration in the presence of 2% (v/v) dimethyl sulphoxide. The higher

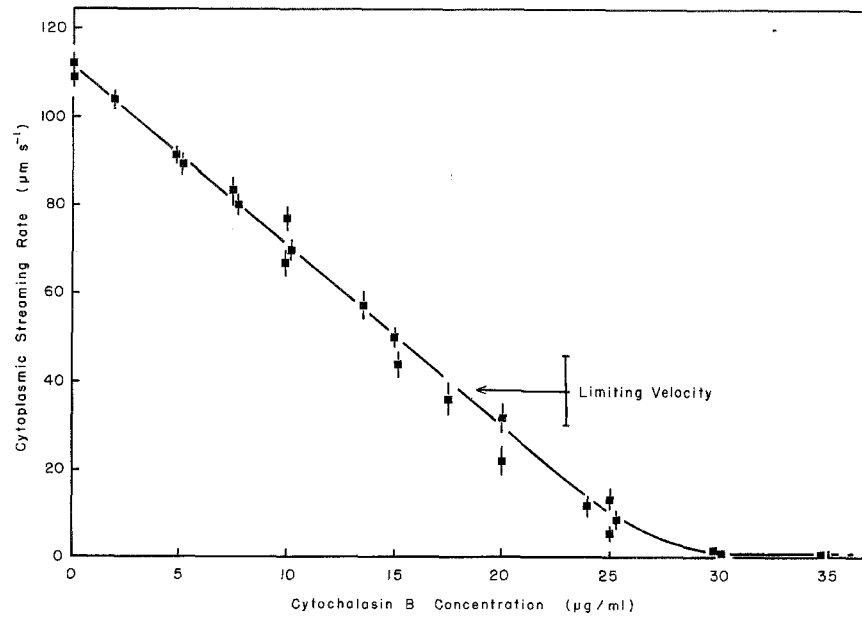

Fig. 4*A*

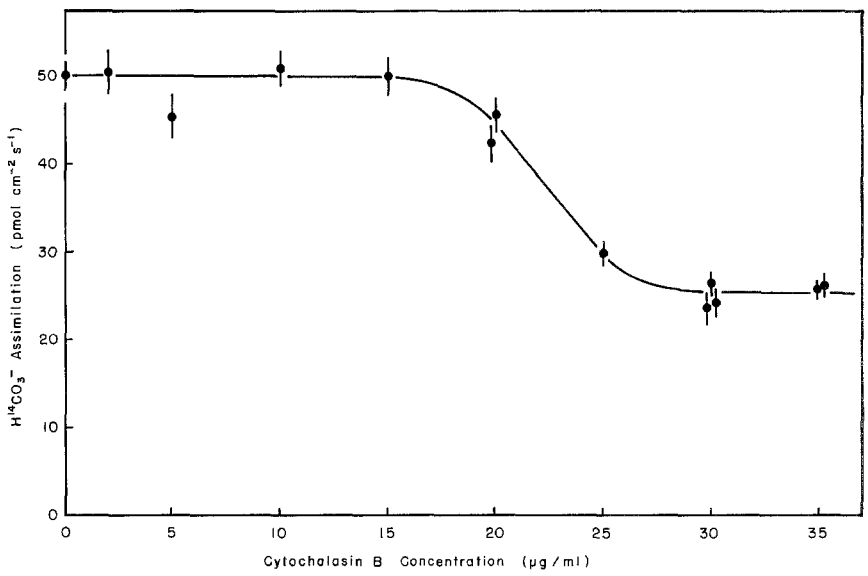

Fig. 4*B*

Fig. 4. Parallel study on the effect of increasing cytochalasin B concentration on cyclosis and $H^{14}CO_3^-$ influx. Experiments were conducted in standard solutions containing 1.0 mM $NaHCO_3$ (pH 9.0), 1% (v/v) dimethyl sulphoxide and the indicated cytochalasin B concentration. All treatments were given 1 hr pre-treatment and experimental periods. Cyclosis (Fig. 4*A*) was measured over the final 10 min of the 1 hr experimental period. Similarly $H^{14}CO_3^-$ was not substituted until this final 10 min period. A check on the cytoplasmic streaming rate was made at the end of $H^{14}CO_3^-$ influx experiments to ensure that rates were compatible with those presented in Fig. 4*A*. The significance of the limiting velocity is explained in the text. All values are expressed as mean ± SEM (10 cells per treatment)

dimethyl sulphoxide level was employed to accelerate the decline in cyclosis. Under these conditions the "limiting streaming velocity" would be attained within 12 ± 3 min compared with 32 ± 8 min associated with the 1% (v/v) dimethyl suphoxide situation (*see* Fig. 2). A theoretical time course of $H^{14}CO_3^-$ influx inhibition in the presence of 2% (v/v) dimethyl sulphoxide was obtained as follows:

(i) From Fig. 4*A* and *B* the percentage inhibition of $H^{14}CO_3^-$ influx was calculated over a range of cyclosis values.

(ii) From the 2% (v/v) dimethyl sulphoxide results presented in Fig.2, and a control $H^{14}CO_3^-$ influx value of 60 pmole per cm^2 per sec, an inhibition curve was computed.

Close agreement between the predicted and experimental curves was obtained (*see* Fig. 5). The depression of $H^{14}CO_3^-$ influx below the predicted level, in the 60–90 min region, may have been due to the increase in dimethyl sulphoxide, *per se*. We consider that these results add weight to our concept of a "limiting cytoplasmic streaming velocity" in relation to the supply of OH^- ions to operational efflux sites.

These results also support our earlier conclusion that cytochalasin B does not affect the membrane-bound $H^{14}CO_3^-$ transport system. This is a significant finding in view of recent reports that indicate cytochalasin B can affect certain membrane-bound active transport processes [3, 8–10]. If the proposal is correct that the cytochalasins inhibit ATP-mediated active transport systems [3, 8], our results imply that $H^{14}CO_3^-$ transport in *C. corallina* may not be energized by ATP.

Partial Inhibition of $H^{14}CO_3^-$ Assimilation by Cytochalasin B

Figs. 4*B* and 5 revealed that when cyclosis was stopped, $H^{14}CO_3^-$ influx and assimilation was only partially inhibited. On the basis of our working hypothesis we expected a close parallel between both the inhibition of cyclosis and $H^{14}CO_3^-$ assimilation. This limited sensitivity of $H^{14}CO_3^-$ assimilation, to the cessation of cyclosis, suggested to us that the normal OH^- efflux system must undergo a modification under these conditions. We conducted cell wall pH scanning experiments to investigate this possibility.

A proliferation of OH^- efflux sites was observed following a 2 hr pretreatment with 30 μg/ml cytochalasin B (Fig. 6*A*). These OH^- efflux sites were considerably smaller and less active when compared with the normal sites developed by the same cell under control conditions. However, the presence of these new OH^- efflux sites explained why $H^{14}CO_3^-$ assimilation was not completely inhibited when cyclosis was stopped.

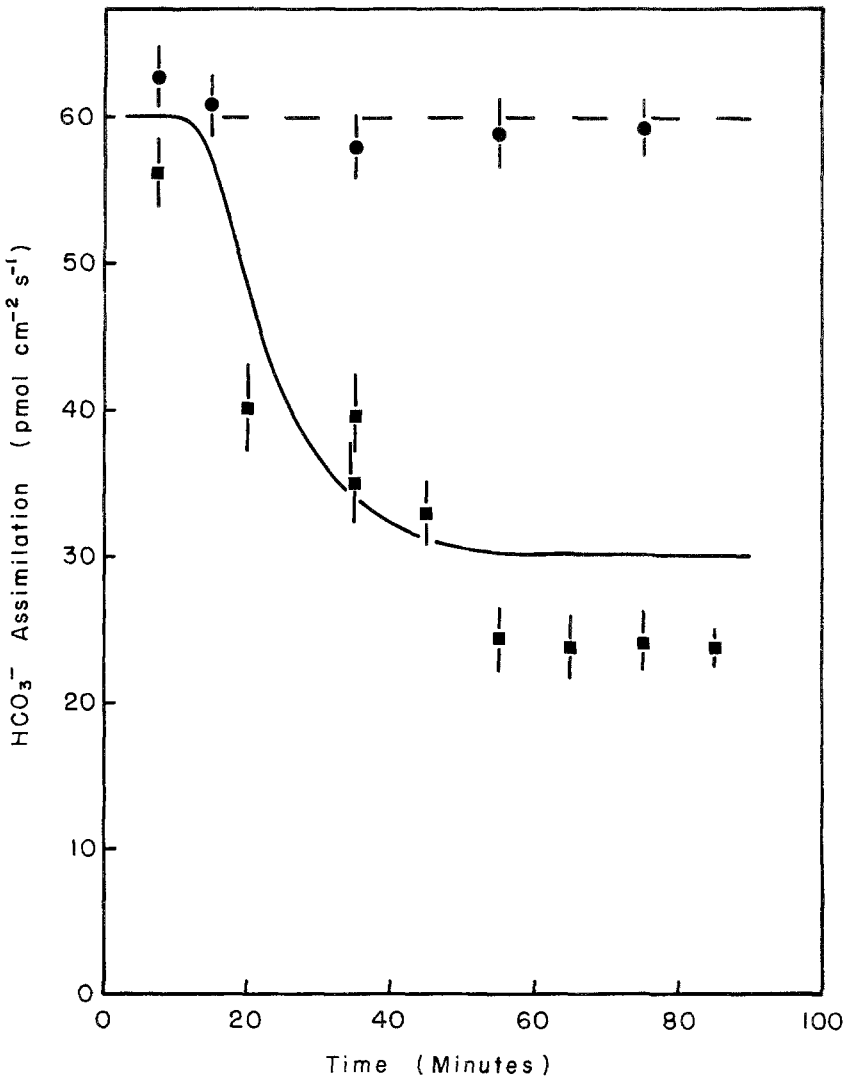

Fig. 5. Comparison between predicted and experimental time courses for $H^{14}CO_3^-$ influx inhibition, in the presence of 30 μg/ml cytochalasin B and 2% (v/v) dimethyl sulphoxide. Experiments were conducted in standard solutions containing 2.0 mM $NaHCO_3$ (pH 9.0). Radioactive $H^{14}CO_3^-$ solutions were employed over the final 10 min experimental period. The symbol (●) and broken line represent the control treatments, conducted in the absence of cytochalasin B. The solid line represents the predicted decay curve based on the limiting cyclosis hypothesis; the values used for its construction were obtained from Figs. 2 and 4 (*see* text for full details). The symbol (■) represents the experimental points. All values are expressed as mean ± SEM (10 cells per treatment)

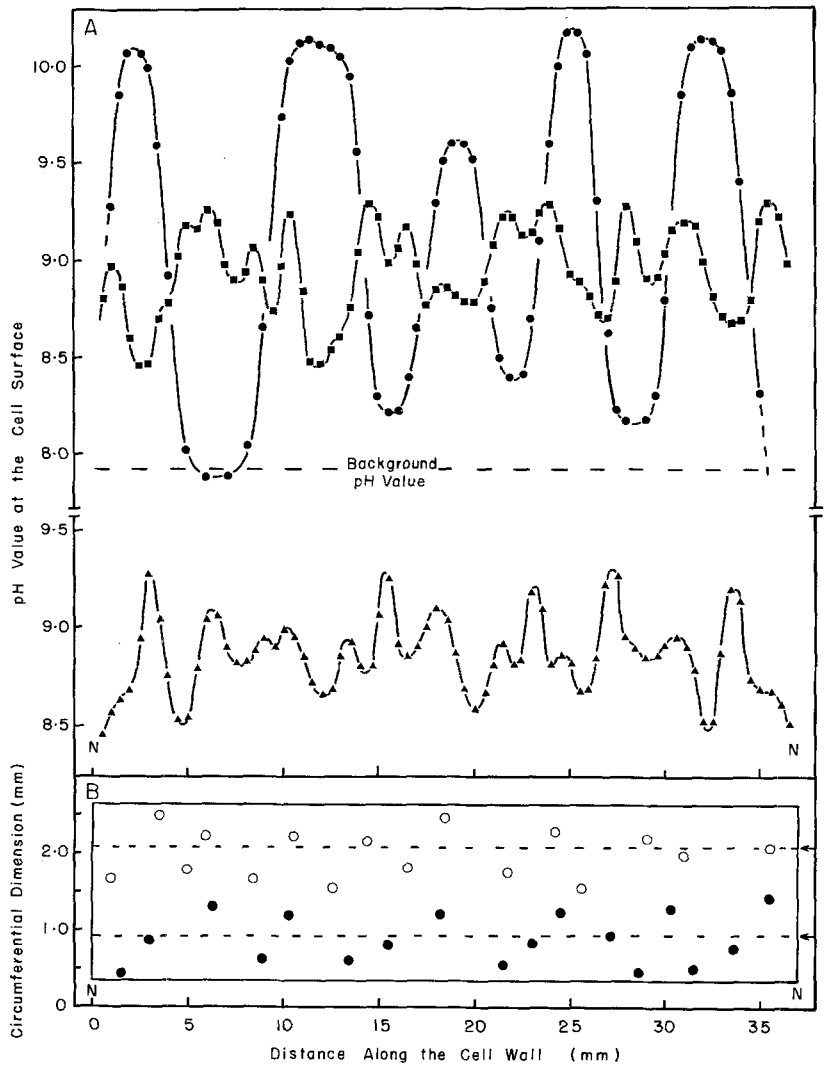

Fig. 6. Influence of 30 μg/ml cytochalasin B on the OH^- efflux pattern established on the internodal cell surface of *C. corallina*. (*A*) The pH value of the agar block and bathing solution was adjusted to 7.9 and the experimental system contained 1.0 mM $NaHCO_3$. Each pH trace was conducted after a 2 hr illumination period (15 Wm^{-2}). The control (●) was conducted and then the cell was transferred to solutions containing 30 μg/ml cytochalasin B. The two cytochalasin B-affected traces, (■) and (▲), were conducted on diametrically opposite cell wall surfaces. Following the completion of the first cytochalasin B trace (■), the experimental cell was transferred to a second identical agar block, and in this block the opposite cell surface was exposed for scanning. The symbol *N* refers to the location of the nodes at the end of this internodal cell. (*B*) The pH pattern developed when cyclosis was stopped by cytochalasin B has been interpreted, and presented in this Fig, in terms of small localized "disc" shaped OH^- efflux sites scattered almost uniformly over the cell surface. The open and closed "discs" are associated with traces (■) and (▲), respectively (*see* text for full details). The arrowed broken lines refer to the two pH scan lines and the rectangle is a two dimensional plan of the internodal cell surface. (The circumference of this internodal cell was 2.3 mm)

It was also found that the location of these new efflux sites bore no relationship to the OH^- efflux sites established during control treatments (*see* Fig. 6*A*). By conducting pH scans along diametrically opposite cell wall surfaces of cytochalasin B treated cells, it was established that these newly developed OH^- efflux sites were very localized indeed. From the two traces presented in Fig. 6*A*, it can be seen that the new sites did not form efflux bands. That is, there was not continuity of the OH^- efflux pattern around the entire cell surface (*cf.* Lucas [11]). Rather, it appeared that the sites exist as small patches of isolated operational carriers (perhaps disc-shaped). If the small pH electrode was traversed through, or close to, the center of an operational "disc" a sharp pH maximum would be registered. However, if the "disc" was to the side of the pH scan line (*see* Fig. 6*B*) a broad peak or shoulder would be registered. The elevation of the pH value above background would also depend upon the distance of the disc from the scan line. The cytochalasin B results of Fig 6*A* have been interpreted in this manner and a possible cell surface distribution of small "disc" OH^- efflux sites is presented in Fig. 6*B*. We wish to stress that we consider this pattern to be very approximate indeed. Since we are uncertain of the circumferential distances over which we can sense these small OH^- efflux sites, it may be that there were many more present than we have shown.

This pattern of small, localized, OH^- efflux sites was confirmed by visual observations using phenol red, an acid/base indicator, in the experimental medium [20]. These experiments were performed by firstly treating internodal cells in a control medium, containing 1.0 mM $NaHCO_3$ (pH 9.0) and 1% (v/v) dimethyl sulphoxide, for 2 hr. Cells were then transferred to an identical solution except that it contained 0.1 mM phenol red and the pH value had been titrated to 5.0. In this medium the normal OH^- banding pattern could be observed as red bands on a yellow background. After recording this pattern, cells were transferred to a solution containing 30 μg/ml cytochalasin B (plus 1.0 mM $NaHCO_3$, pH 9.0 and 1% dimethyl sulphoxide). Following a 2 hr treatment in this solution the streaming rate was checked to ensure cyclosis had been inhibited and then the cells were transferred to an identical solution (containing 0.1 mM phenol red), pH value 5.0. Under these conditions the pattern of small localized OH^- efflux sites could be readily observed and the number of sites recorded. As many as 30–50 sites could be counted on a cell of length 3–4 cm.

The ability of these cells to establish this new OH^- efflux pattern, when cyclosis is stopped, demonstrates that the OH^- carriers cannot

be restricted to a limited number of discrete bands along the plasmalemma length. Consequently we had to modify our working hypothesis. Our experimental results suggest the OH^- efflux carriers are rather uniformly distributed within the cell's total plasmalemma surface, i.e., in a similar manner to that proposed for the HCO_3^- carriers. At any one time, however, only a small fraction of these carriers are operational. Undoubtedly the cellular mechanism that determines which carriers become operational will also determine the location and form of these sites along the cell surface.

A Possible Cytoplasmic Mechanism for Determining the Spatial Distribution of Operational OH^- Sites Along the Cell Length

As yet we have no information regarding the molecular nature of the OH^- carriers or their operational sites within the plasmalemma. Consequently our model is formulated on very generalized concepts of possible interactions between the cellular processes of photosynthesis, cyclosis and OH^- efflux. The model is presented in terms of a description of the sequential events which are considered to occur in the cytoplasmic phase following cell illumination.

(i) The commencement of photosynthesis generates OH^- ions within the chloroplast layer.

(ii) These OH^- ions diffuse into the cortical (gel) and streaming cytoplasm. Cyclosis and the short diffusion time between the two cytoplasmic phases results in a uniform "concentration" of OH^- throughout the nonmembrane bounded regions of the cytoplasm. (It should be noted that we do not wish to specify, at this stage, OH^- *per se* or a substrate which generates OH^- at the efflux carrier site.)

(iii) The OH^- "concentration" increases until the activating level of the primary OH^- efflux site is reached [12]. (There must be a cellular mechanism which, under normal cyclosis conditions, imparts not only this hierarchical status to these respective sites, but also causes the operational entities to exist in the form of OH^- efflux bands. This mechanism has not been fully elucidated [12].)

(iv) Activation of the primary site reduces the OH^- "concentration" in its immediate vicinity. The localized concentration decrease will, however, be relatively small due to the coupling between this region and the larger "pool" of OH^- in the streaming cytoplasm.

(v) If the efflux rate through the primary site is less than the total cellular rate OH^- generation by the chloroplasts, the cytoplasmic OH^-

"concentration" will increase with time. This increase will be slightly greater in the cortical cytoplasmic regions farthest from the primary efflux site. It is in this region that the sub-primary site is generally found (*see* Lucas [12], Fig. 2), and it will activate once its activating concentration has been attained.

(vi) Further OH^- efflux sites will activate only if the cytoplasmic OH^- "concentration" continues to increase. The plasmalemma contains a macroscopic continuum of OH^- efflux carriers which can, under the correct conditions, form subsidiary efflux sites. Hence, subsidiary sites will become activated at those locations along the cell length where the OH^- "concentration" has increased to the subsidiary activating level.

(vii) In conjunction with (vi), it should be stressed that the increase in OH^- "concentration" will be greatest in the cortical cytoplasmic regions having the greatest distance separating consecutive operational OH^- efflux sites. This physical feature of the system will cause the OH^- efflux sites to be spaced at almost regular intervals along the cell length.

(viii) The number of operational OH^- efflux sites increases until the efflux through these sites establishes a steady state OH^- "concentration" in the cytoplasmic phase. There is, however, a limit to the number of OH^- sites that can operate along any one cell. This limit is related to the inhibition of the HCO_3^- carriers by CO_3^{2-}, at pH values above 9.6 [13]. Since the pH value within the immediate cell wall region of an operational OH^- band is generally 9.5–10.1, it is obvious that this region of plasmalemma would not be available for HCO_3^- transport. Hence, the more bands operating, the smaller is the area available for HCO_3^- transport. In the steady state, under saturating exogenous HCO_3^- conditions, there exists a balance between maximizing HCO_3^- influx and the area of plasmalemma required to dispose of the OH^- generated by this HCO_3^- influx.

When cyclosis is stopped, or reduced to a very low level, the cell loses its fine control over cytoplasmic pH regulation. Under these conditions one might expect the OH^- "concentration" in the cytoplasm to increase to such a level that a "continuum" of subsidiary bands (sites) would become activated along the entire cell length. The fact that this was not observed experimentally suggests that when cyclosis was inhibited, the cellular mechanism that imparts status, etc., to these sites is also impaired. The network of small "disc" efflux sites which was established appeared, however, to cope quite adequately with the imposed

limitations of OH^- diffusion. This network pattern may reflect an attempt to minimize the OH^- diffusion path whilst leaving a reasonable area of plasmalemma available for HCO_3^- transport.

A network pattern of this nature is in fact rather reminiscent of $CaCO_3$ deposition in the more primitive members of the Characeae (genus Tolypella [17]). Future studies relating to the implications of this change in basic OH^- efflux pattern, in terms of the phylogeny of the Characeae, may provide independent support for phylogenetic arguments presently based on anatomical and cytological data [17, 18, 24].

Conclusions

In this study we have shown that the OH^- transport system of *C. corallina* is not localized at discrete sites along the plasmalemma. A macroscopic continuum of potentially operational OH^- carriers within the cell's plasmalemma appears to be a more accurate description of this OH^- efflux system. The experiments described also firmly established that the streaming cytoplasm is the mode by which the OH^- are delivered from the chloroplasts to the operational efflux sites, under normal conditions.

We feel that our descriptive model can account for the experimentally observed features of the total OH^- efflux system of *C. corallina*. However, the limitations of this model are all too apparent. We will not have a complete characterization of this phenomenon until we have elucidated the features of this system at the molecular level. This will certainly provide an interesting avenue for future research.

This work was supported jointly by grants from the National Research Council of Canada (grant No. A6459) and the Connaught Fund (University of Toronto).

References

1. Aldridge, D.C., Armstrong, J.J., Speake, R.N., Turner, W.B. 1967. The structure of cytochalasins A and B. *J. Chem. Soc. C* **2**:1667
2. Bradley, M.O. 1973. Microfilaments and cytoplasmic streaming: Inhibition of streaming with cytochalasin. *J. Cell Sci.* **12**:327
3. Bos, C.J., Emmelot, P. 1974. Studies on plasma membranes: XXI. Inhibition of liver plasma membrane enzymes by tumor-promoting phorbolester, mitotic inhibitors and cytochalasin B. *Chem. Biol. Interact.* **8**:349
4. Chen, J.C.W. 1973. Observations of protoplasmic behaviour and motile protoplasmic fibrils in cytochalasin B treated *Nitella* rhizoid. *Protoplasma* **77**:427
5. Costerton, J.W.F., MacRobbie, E.A.C. 1970. Ultrastructure of *Nitella translucens* in relation to ion transport. *J. Exp. Bot.* **21**:535

6. Hepler, P.K., Palevitz, B.A. 1974. Microtubules and microfilaments. *Annu. Rev. Plant Physiol.* **25**:309
7. Kamiya, N. 1960. Physics and chemistry of protoplasmic streaming. *Annu. Rev. Plant Physiol.* **11**:323
98. Kuo, S.C., Lampen, J.O. 1975. Action of cytochalasin A, a sulfhydryl-reactive agent, on sugar metabolism and membrane-bound adenosine triphosphatase of yeast. *Biochim. Biophys. Acta* **389**:145
9. Lin, S., Spudich, J.A. 1974. Biochemical studies on the mode of action of cytochalasin B: Cytochalasin B binding to red cell membranes in relation to glucose transport. *J. Biol. Chem.* **249**:5778
10. Lin, S., Spudich, J.A. 1974. Binding of cytochalasin B to a red cell membrane protein. *Biochem. Biophys. Res. Commun.* **61**:1471
11. Lucas, W.J. 1975. Analysis of the diffusion symmetry developed by the alkaline and acid bands which form at the surface of *Chara corallina* cells. *J. Exp. Bot.* **26**:271
12. Lucas, W.J. 1975. The influence of light intensity on the activation and operation of the hydroxyl efflux system of *Chara corallina*. *J. Exp. Bot.* **26**:347
13. Lucas, W.J. 1975. Photosynthetic fixation of ^{14}carbon by internodal cells of *Chara corallina*. *J. Exp. Bot.* **26**:331
14. Lucas, W.J. 1976. Plasmalemma transport of HCO_3^- and OH^- in *Chara corallina:* Nonantiporter systems. *J. Exp. Bot.* **27**:19
15. Lucas, W.J., Smith, F.A. 1973. The formation of alkaline and acid regions at the surface of *Chara corallina* cells. *J. Exp. Bot.* **24**:1
16. Lucas, W.J., Smith, F.A. 1976. Influence of irradiance on H^+ efflux and Cl^- influx in *Chara corallina:* An investigation aimed at testing two Cl^- transport models. *Aust. J. Plant Physiol.* **3**:1
17. Sawa, T. 1974. New chromosome numbers for the genus *Tolypella* (Characeae). *Bull. Torrey Bot. Club* **101**:21
18. Sawa, T., Frame, P.W. 1974. Comparative anatomy of Charophyta: I. Oogonia and Oospores of *Tolypella,* with special references to the sterile Oogonial cell. *Bull. Torrey Bot. Club* **101**:136
19. Smith, F.A. 1970. The mechanism of chloride transport in Characean cells. *New Phytol.* **69**:903
20. Spear, D.G., Barr, J.K., Barr, C.E. 1969. Localization of hydrogen ion and chloride ion fluxes in *Nitella*. *J. Gen. Physiol.* **54**:397
21. Wessell, N.K., Spooner, B.S., Ash, J.F., Bradley, M.O., Luduena, M.A., Taylor, E.L., Wrenn, J.T., Yamada, K.M. 1971. Microfilaments in cellular and developmental processes. *Science* **171**:135
22. Williamson, R.E. 1972. A light-microscope study of the action of cytochalasin B on the cells and isolated cytoplasm of the Characeae. *J. Cell Sci.* **10**:811
23. Williamson, R.E. 1975. Cytoplasmic streaming in *Chara:* A cell model activated by ATP and inhibited by cytochalasin B. *J. Cell Sci.* **17**:655
24. Wood, R.D., Imahori, K. 1965. A revision of the Characeae, Part I. J. Cramer, Weinheim